Journal of Applied Polymer Science

The Effect of Formaldehyde/Phenol (*F*/*P*) Molar Ratios on Function and Curing Kinetics of High-Solid Resol Phenolic Resins

Yufeng Ma,[1,2,3,4] Wei Zhang,[1,2,3,4] Chunpeng Wang,[1,2,3,4] Yuzhi Xu,[1,2,3,4] Fuxiang Chu[5]

[1]Institute of Chemical Industry of Forestry Products, CAF, Jiangsu Province; Nanjing 210042, China
[2]National Engineering Lab. for Biomass Chemical Utilization, Jiangsu Province; Nanjing 210042, China
[3]Key and Open Lab. on Forest Chemical Engineering, SFA, Jiangsu Province; Nanjing 210042, China
[4]Key Lab. of Biomass Energy and Material, Jiangsu Province; Nanjing 210042, China
[5]Chinese Academy of Forestry, Beijing 100091, China
Correspondence to: F. Chu (E-mail: chufuxiang@caf.ac.cn) or C. Wang (E-mail: wangcpg@163.com)

ABSTRACT: A series of high-solid resol phenolic resins (HSRPRs) were synthesized with different molar ratios (1.6, 1.8, 2.0, 2.2, and 2.4) of formaldehyde to phenol using calcium oxide and sodium hydroxide as catalyst. The effects of *F*/*P* molar ratios on physical properties, free formaldehyde and phenol, activity, structure, and thermally resistant properties of HSRPRs were fully investigated by chemical assays, liquid and solid ^{13}C-NMR, Fourier transform infrared spectroscopy, and thermogravimetric analysis. The curing kinetics of different *F*/*P* molar ratios were explored with differential scanning calorimeter at four different heating rates (5, 10, 15, 20°C/min) from 35 to 200°C. Overall, HSRPRs with $F/P = 2.0$ had excellent comprehensive properties. The study was significant in solving the wastewater problem during the process of industry-scale preparation of HSRPRs. We believed that the experimental findings would provide a new avenue for further study and application of HSRPRs. © 2013 Wiley Periodicals, Inc. J. Appl. Polym. Sci. 129: 3096–3103, 2013

KEYWORDS: thermosets; thermogravimetric analysis (TGA); differential scanning calorimetry (DSC)

Received 9 August 2012; accepted 23 November 2012; published online 18 February 2013
DOI: 10.1002/app.38869

INTRODUCTION

In recent years, the fire of high-rise building occurred frequently in China, and caused tremendous property damages and human casualties. Most of fires were caused due to the use of flammable insulation materials. Especially these flammable foams generated toxic gases during combustion, which lowered the survival of human beings.[1] However as a kind of excellent flame retardant thermal insulation material, phenolic foam has many advantageous features, such as, excellent flame resistance and thermal stability, low smoke density and toxicity, no dripping of molten plastic during combustion, low thermal conductivity, and high resistance to chemicals and solvents.[1–5] Because of these reasons, phenolic foam has reignited people's interest. It is widely used in the fields of agriculture, horticulture, buildings, ships, and aircraft with promising developments in materials.[3,6]

High-solid resol phenolic resins (HSRPRs, solid content 70–85%) are the raw materials necessary in the preparation of phenolic foam. Traditional resol phenolic resins (TRPRs) (solid content 40–50%) are synthesized using the content of about 37% formaldehyde solution as monomer. However, in order to achieve the properties of HSRPRs, TRPRs need to be dehydrated. During the dehydration, a large amount of industrial wastewater is inevitably generated.[7] Normally, 500 kg waste water is generated during the production of 1.0 metricton HSRPRs. The phenol content in such waste water is about 6.6×10^4 mg/L, much greater than the standard phenol content (less than 1 mg/L).[8]

To reduce the generation of such toxic waster water, there have been many efforts toward solving this problem. The most effective strategy is using paraformaldehyde replacing formaldehyde. Liu et al.[9,10] synthesized a boron-containing phenolic resin (BPFR) using paraformaldehyde, and studied the curing reaction, thermal properties, and stability of BPFR by Fourier transform infrared (FTIR), differential scanning calorimeter (DSC), thermogravimetric analysis (TGA), and torsional braid analysis. Park et al.[11,12] prepared phenol formaldehyde (PF) resin using *para*-formaldehyde, and investigated the cure-acceleration effects of three carbonates on liquid and cured PF resins by thermomechanical analysis, DSC, liquid and solid-state ^{13}C-NMR spectroscopies. However, these works lacked a comprehensive investigation in using *para*-formaldehyde to prepare HSRPRs and evaluate their properties.

In this article, 37% formaldehyde solution and paraformaldehyde (ω = 1/1.57–1/3.18) were mixed to synthesize a series of HSRPRs with different *F*/*P* molar ratios (1.6, 1.8, 2.0, 2.2, and 2.4), resulting in solid content in the range of 74–80%. The effects of *F*/*P* molar ratios on the physical properties, the content of free formaldehyde and phenol, the activity, structure, thermally resistant properties, and curing kinetics were studied by chemical analysis, ^{13}C-NMR, FTIR, TGA, and DSC. This is the first report utilizing a self of experimental parameters and characterization tool to study the synthesis and properties of HSRPRs, and the purpose was to minimize wastewater generation.

MATERIALS AND METHODS

Materials

Phenol(>99%), formaldehyde (37% wt % aqueous solution), calcium oxide, and sodium hydroxide were obtained from Nanjing Chemical Reagent, Ltd. Paraformaldehyde (≥95%) was obtained from Shanghai Lingfeng chemical Reagent. Other materials were commercial products.

Synthesis of HSRPRs

In the synthesis of HSRPRs, phenol, formaldehyde aqueous solution (37%), paraformaldehyde, calcium oxide, and sodium hydroxide solution (50%) were used directly as received without further purification. Phenol, formaldehyde, and paraformaldehyde were charged into the reaction vessel according to the calculated amounts, in which only the total amount of phenol and formaldehyde aqueous solution was added at this time, and a calculated amount of calcium oxide was dropped slowly into the vessel for 30–40 min under continued stirring at 85°C. The first part of *para*-formaldehyde and sodium hydroxide aqueous solution were then added into the reactor and kept for 50–70 min at 85°C. Then the second parts of them were added according to the first step. Finally, the third part of sodium hydroxide aqueous solution was added to the reactor, and the temperature was kept at 75°C for 15–20 min. After that, the system was cooled down to 40–50°C, by adding ice water. The HSRPRs was obtained, and the solid content of all synthesized HSRPRs was about 70–80% (W_t) based on oven-dry measurement.

HSRPRs were defined as R/1.6, R/1.8, R/2.0, R/2.2, and R/2.4, where 1.6, 1.8, 2.0, 2.2, and 2.4 represented the *F*/*P* molar ratios used in this work. The *F*/*P* molar ratios were checked by measuring free phenol and formaldehyde in HSRPRs.

Chemical and Physical Methods

The solid contents of HSRPRs were measured according to BS EN 827-1995. The viscosities were obtained in accordance with ASTM D1084-1997. The free phenol contents were measured according to ASTM D1312-93. The free formaldehyde contents were measured according to DIN EN ISO 9397-1997. The gel time was determined by ISO 9396:1997. The methylol contents were measured according to ISO 8989-1995.

FTIR Measurements

FTIR measurements were performed using freeze-dried samples and cured samples (120°C, 2 h). The analysis was carried out with a FTIR spectrometer (Nicolet IS10, USA). The background spectrum was measured for automatic background subtraction.

TGA Measurements

TGA was used to study the thermal stability and degradation of HSRPRs. TGA spectra were recorded on NETZSCH (Germany) STA 409 thermogravimetric apparatus. Each cured sample was placed on a balance located in the furnace with the temperature range from 35°C to 600°C at a heating rate of 15°C/min in flowing nitrogen atmosphere (20 mL/min). The thermograms of weight loss versus temperature were obtained to show the different degradation processes. The experiments were performed in triplicate and the considered values were averaged from those of three runs (the maximum difference between the average and the experimental values being within ±1°C).

Liquid ^{13}C-NMR Measurements

Liquid ^{13}C-NMR spectra were obtained on a Bruker (Switzerland) DRX 500 NMR spectrometer. The spectra were recorded under the following conditions: a relaxation delay of 6 s with gated Waltz-16 1H decoupling during the acquisition period. About 24,000 scans were accumulated for each spectrum, and spectral width was 300 ppm. Each sample was dissolved directly in deuterated water for ^{13}C-NMR tests. ^{13}C chemical shift was measured with respect to tetramethylsilane (TMS) as the internal standard.

Solid ^{13}C-NMR Measurements

Solid-state ^{13}C-NMR spectra of each cured sample (120°C, 2 h) were obtained on a Bruker (Switzerland) DRX 500 NMR spectrometer at a frequency of 100 MHz. Chemical shift was calculated relative to TMS for NMR control. Acquisition time was 0.015 s. All spectra run with a relaxation delay of 6 s and were accurate to 1 ppm with a PC time of 0.2 ms and spectral width of 300 ppm.

DSC Measurements

DSC spectra were obtained on Diamond DSC (PerkinElmer, USA). DSC measurements were performed using freeze-dried samples of about 5.0 × 10^3 g. Heating rates were 5, 10, 15, and 20°C/min. The scanning temperature ranged from 25 to 200°C in flowing nitrogen atmosphere (0.02 L/min).

RESULTS AND DISCUSSION

Physical Properties Studies

The HSRPRs were synthesized under alkaline condition. A variety of hydroxyl cresol was generated during addition reaction between formaldehyde and phenol. Meanwhile, a mixture of unitary and multivariate phenolic alcohols was formed. With the ratios of *F*/*P* molar ratios increased, the fraction of unitary and multivariate phenolic alcohols increased, and the degree of polycondensation was enhanced. Along with the continuous polycondensation reaction, the viscosity and solid content of HSRPRs increased with the increase of *F*/*P* molar ratios.[13–15] The effect of the *F*/*P* molar ratios on the viscosity and solid content is shown in Figure 1.

The solid content was closely related to the synthetic formula. During the synthetic process of HSRPRs, the content of formaldehyde (37 wt %) and phenol was unchanged, but the content of paraformaldehyde increased gradually with the increase of the *F*/*P* molar ratios. Therefore, the solid content increased dramatically as $F/P \leq 2.2$. However, when $F/P \geq 2.2$, the reaction might reach the equilibrium state, further addition of paraformaldehyde did not participate in reactions, so the solid content

Applied Polymer SCIENCE

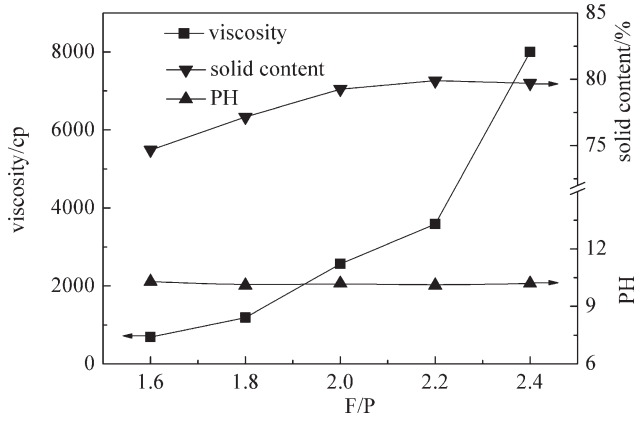

Figure 1. The viscosity, PH value, and solid content of HSRPRs using different *F*/*P* molar ratios.

was almost constant. This was indirectly confirmed by the content of free formaldehyde of HSRPRs which increased much fast as the $F/P \geq 2.2$ (Figure 2).

The viscosity of HSRPRs was closely related to the solid content and pH of HSRPRs. The pH values were nearly unchanged with the increase of *F*/*P* molar ratios; therefore, the viscosity was mainly affected by the solid content. The viscosity increased with the increase of the solid content. High viscosity would affect the processability of HSRPRs. Considering all these, the best properties were achieved when the *F*/*P* molar ratios was 2.0, the viscosity was 2567 mPa s, and the solid content was 79.25%.

Free Formaldehyde and Phenol

Phenol and formaldehyde are volatile toxic substances. During the synthetic process of HSRPRs, it would be harmful to humans and the environment, if formaldehyde and phenol didn't consume. It is vital to choose suitable *F*/*P* molar ratios to control the reaction process and to reduce the residual content of toxic substances.[15–18]

The effect of the *F*/*P* molar ratios on the free formaldehyde and free phenol of HSRPRs is shown in Figure 2. With the *F*/*P* molar ratios increased, hydroxymethylation reaction occurred between formaldehyde and the *ortho* and *para* hydrogen of phenolic-hydroxyl, meanwhile poly-condensation and crosslinking reactions occurred among the active sites of benzene ring, resulting in a decrease of the free phenol concentration. However, the free formaldehyde concentration increased with the increase of *F*/*P* molar ratios. When the *F*/*P* molar ratio was less than 2.0, the reaction was more complete between formaldehyde and phenol. The free formaldehyde concentration was low, and maintained below 0.86. As the *F*/*P* molar ratio was less than or equal to 2.0, the content of unreacted formaldehyde increased gradually. However the content of free formaldehyde increased much fast, when the *F*/*P* molar ratio was greater than or equal to 2.0. Therefore the content of free formaldehyde and free phenol could be controlled by the *F*/*P* molar ratios to obtain the low content of residual toxic substances inside the resin. Figure 2 showed that both free formaldehyde and free phenol were maintained at a relatively low level as the *F*/*P* molar ratio was 2.0, with the content of free formaldehyde at 0.86%, and the content of free phenol at 3.01%.

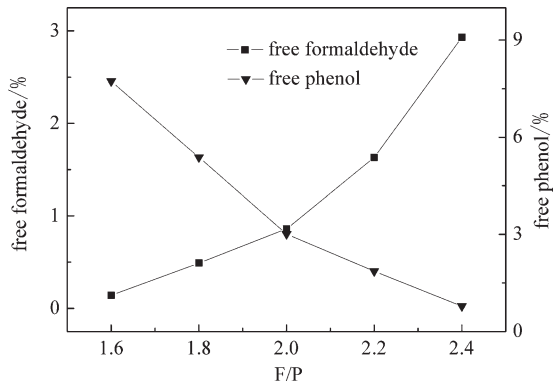

Figure 2. The free formaldehyde and phenol of HSRPRs using different *F*/*P* molar ratios.

The Activity Studies

The active sites of resins were the *ortho* and *para* of phenolichydroxyl and hydroxymethyl groups. Hydroxymethyl groups had higher reaction activity. The active groups' concentration of resin was measured by titration to reflect the resins activity.[18,19] The depolymerization reaction of paraformaldehyde generated formaldehyde. At the same time, the addition reaction occurred between *ortho* and *para* of phenolichydroxyl and formaldehyde, generating the *ortho* or *para* hydroxymethyl phenol. Thus, the hydroxymethyl concentration increased continuously, and the resins activity increased accordingly. The effect of the *F*/*P* molar ratios on hydroxymethyl concentration of HSRPRs is shown in Figure 3. With the *F*/*P* molar ratios increasing, the concentration of hydroxymethyl increased gradually, indicating the increased activity of the resin.

Structure Analysis of Uncured HSRPRs

Figure 4 shows the FTIR spectra of uncured HSRPRs, and the FTIR signals could be assigned according to the previous literature.[20–25] With the increase of *F*/*P* molar ratios, the hydroxymethyl absorption peak near 1020 cm^{-1} of benzene ring, the ether bond (near 1146 cm^{-1}) and the *ortho–para′* substituted

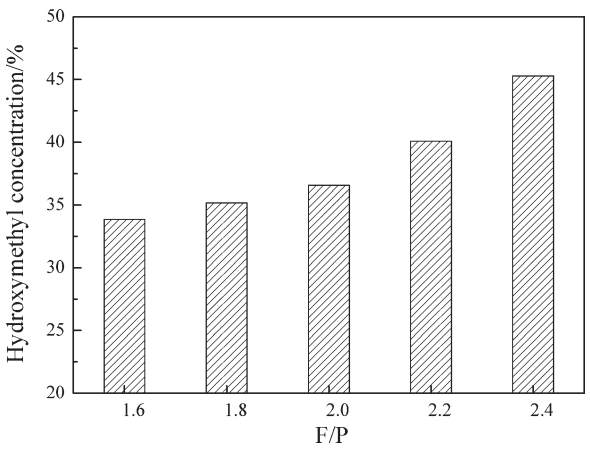

Figure 3. The hydroxymethyl concentration of HSRPRs using different *F*/*P* molar ratios.

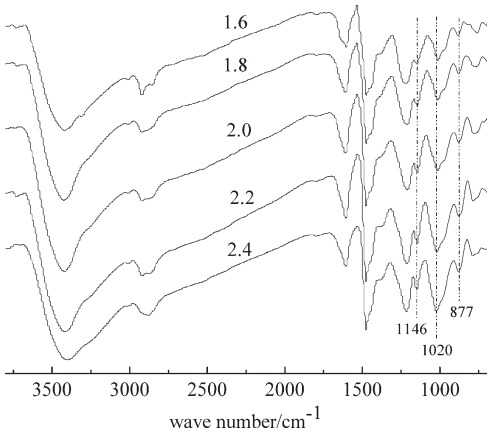

Figure 4. The FTIR spectra of the uncured HSRPRs using different *F*/*P* molar ratios.

benzene (near 877 cm^{-1}) were enhanced gradually. Figure 5 shows the ^{13}C-NMR of uncured HSRPRs, and the ^{13}C-NMR shifts and group assignments are listed in Table I. The methylol positions were also increased. The signals of dimethylene ether bridges were almost not detected as the *F*/*P* molar ratios was less than 2.0, and then increased slightly. The free *ortho* and *para* positions decreased, and the unsubstituted *para* positions decreased even more rapidly than the *ortho* ones. During the addition reactions and polycondensation reactions, the activity of *para* phenol-hydroxyl was higher than that of the *ortho*. On the other hand, due to steric hindrance and hydrogen bonds, the *ortho* keto-form structures were difficult to participate in reaction comparing with the *para*. Therefore, at the low molar ratio, the *ortho* of phenol-hydroxyl was difficult to substitute compared with the *para*, and its absorption intensity was weaker. But with the increase of *F*/*P* molar ratios, the addition reactions were promoted between formaldehyde and the *ortho*/*para* of phenol-hydroxyl. Hydroxymethylation reactions were also enhanced. Meanwhile the poly-condensation reactions were intensified. The quantity of hydroxymethyl and methylene bridges bonds increased, therefore the substituted probability of the active hydrogen of the *ortho*/*para* phenol-hydroxyl groups increased. Meanwhile there were two *ortho* of phenol-hydroxyl, therefore the substituted probability of the *ortho* hydrogen of

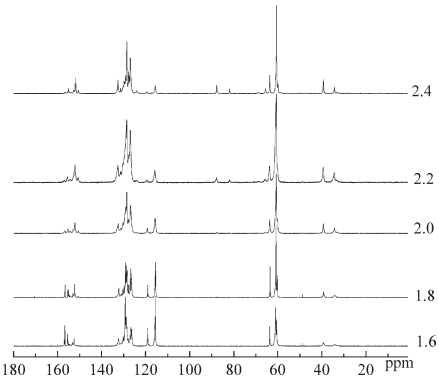

Figure 5. The ^{13}C-NMR spectra of the uncured HSRPRs using different *F*/*P* molar ratios.

Table I. ^{13}C-NMR Chemical Shifts of HSRPRs[18,26–32]

	Chemical shifts (ppm)	
Assignment of the carbons	Uncured	Cured
Methylene bridges	33.04–39.30	34.39–37.08
Methanol	48.78–48.82	
Methylol	59.89–63.64	57.60–70.47
Dimethylene ether bridges	65.47–68.90	90.53
Oxymethylene of formaldehyde oligomers	81.82–81.90	
Phenolic hemiformals	87.81–87.73	
Free ortho/ para	115.53–119.40	
Meta, substituted ortho/ para	124.03–132.58	129.62–129.92
Phenoxy region	150.51–156.98	150.98–151.60
Phenoxy, alkylated in ortho region	154.24–155.49	
Phenoxy, alkylated in para region	156.57–156.98	
Formate, bicarbonate, and carbonate species		171.62

phenol-hydroxyl groups was more than the *para* ones. But with reactions continuing, the *para* of phenol-hydroxyl was almost substituted completely. Therefore, the absorption intensity of unsubstituted *ortho* and *para* of benzene ring gradually weakened. The absorption intensity of substituted *ortho* increased obviously, but the *para* substituted increased slightly, and then remained constant.

Structure Analysis of Cured HSRPRs

The primary curing reaction of resol phenolic resins had two types[33] (Figure 6): (1) the condensation reactions could occur between hydroxymethyl of phenolic nuclear and the *ortho*/*para* hydrogen of other phenol nucleus, in which methylene was generated. (2) The curing reactions also occurred among the hydroxymethyl from different phenol nucleus, and water was produced to generate dibenzyl ether.

The FTIR spectra of cured HSRPRs are shown in Figure 7, and the FTIR signals could be assigned with the previous literature.[34–36] With the increase of *F*/*P* molar ratios, the stretching vibration absorption peak of hydroxymethyl (near 1030 cm^{-1}) was enhanced. When the *F*/*P* molar ratio was less than 2.0, the absorption peak of ether bonds (near 1146 cm^{-1}) was almost constant, and the scissor vibration absorption peak of methylene (near 1360 cm^{-1}) was almost not detected. When the *F*/*P* molar ratio was more than or equal to 2.0, the absorption peak of ether bonds slightly increased, and the scissor vibration absorption peak of methylene was enhanced obviously. The effect of the *F*/*P* molar ratios on ^{13}C-NMR of cured HSRPRs is

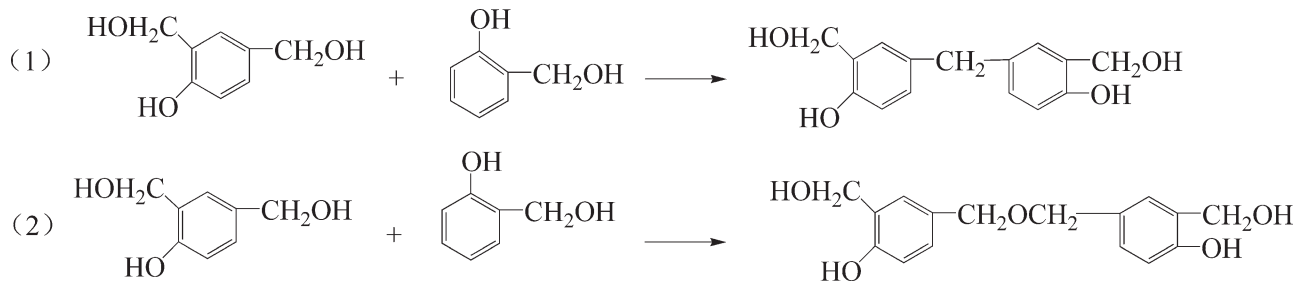

Figure 6. The primary curing reactions of resol phenolic resins.

shown in Figure 8, and the ^{13}C-NMR shifts and group assignments are assigned in Table I. With the *F*/*P* molar ratios increased, the absorption peak intensity of the *ortho*/*para* methylol and methylene increased slightly. At the low molar ratio, the dimethylene ether bridge was almost undetected. When the *F*/*P* molar ratio was more than 2.0, only a weak absorption peak appeared. Another peak appeared at 171 ppm, which was assigned to carbonate and formate ions. Formaldehyde was decomposed by the Cannizzaro reaction to formic acid and methanol and to hydrogen and formic acid by other base-catalyzed reactions. Formic acid further decomposed to carbonate and bicarbonate ions, in accordance with published results.[29] These results indicated that at the low molar ratio, the primary curing reaction was the condensation reaction between hydroxymethyl from benzene ring and the *ortho*/*para* hydrogen from other benzene rings, in which methylene was generated. But at high molar ratio, the curing reaction also occurred among the hydroxymethyl of different benzene ring, and a small amount of water was produced, generating dibenzyl ether.

TGA Studies

The effect of *F*/*P* molar ratios on the TGA and DTG of HSRPRs is shown in Figure 9. As it was previously reported in the literature,[37–40] the process of thermal decomposition can be grouped into three different stages. The first stage was 35–320°C. The weight loss was relatively low, mainly due to the release of excess phenol, formaldehyde, short oligomers, and water. The second stage of the thermal decomposition was within the range of 320–470°C. The pyrolysis and the polymerization reactions of pyrolysis products started to occur, but it was not the main thermal degradation stage. The main process of thermal degradation was in the third stage in the range of 470–600°C, which was the process of rapid thermal degradation of HSRPRs, where most weight loss might be caused by chain scission and resin decomposition, resulting in fragmentation of the resin into low molecular weight products.

The initial decomposition temperatures (T_i), which are often considered as a parameter to evaluate the thermal stability of polymers, can be obtained by the TG curves as the intersection between the starting mass line and the maximum gradient tangent to the TG curve. The compound with higher T_i was considered more thermally stable.[41–44] The *F*/*P* molar ratios of HSRPRs was 1.6, 1.8, 2.0, 2.2, and 2.4, and T_i values were 142.3°C, 160.7°C, 165.9°C, 161.8°C, and 164.9°C, respectively. But with the increase of *F*/*P* molar ratios, the residue (600°C) of HSRPRs was decreased gradually, which was 73.92%, 68.11%, 65.10%, 61.12%, and 59.12%, respectively. These results showed that the thermal stability was the highest when the *F*/*P* molar ratio was 2.0. While thermal stability at high temperature was gradually decreased with the *F*/*P* molar ratios increasing.

The Curing Kinetics Studies

The DSC curves were analyzed from peak shape and temperature. Values for E_a were obtained according to Kissinger's equation [eq. (1)],[45] and the relationship among the curing

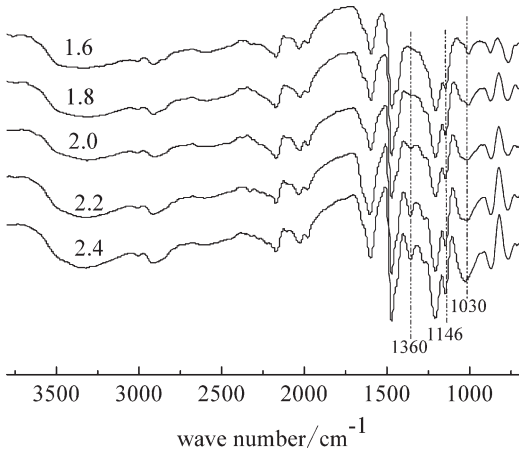

Figure 7. The FTIR spectra of the cured HSRPRs using different *F*/*P* molar ratios.

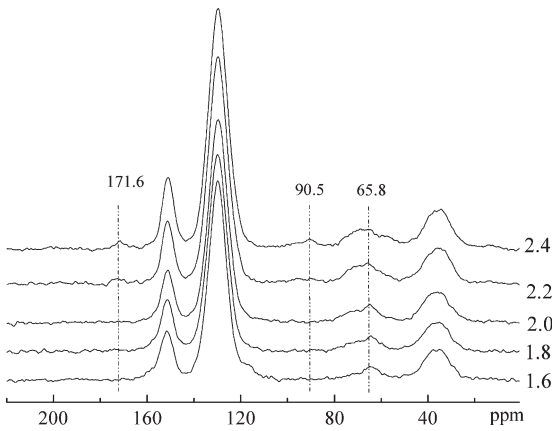

Figure 8. The ^{13}C-NMR spectra of the cured HSRPRs using different *F*/*P* molar ratios.

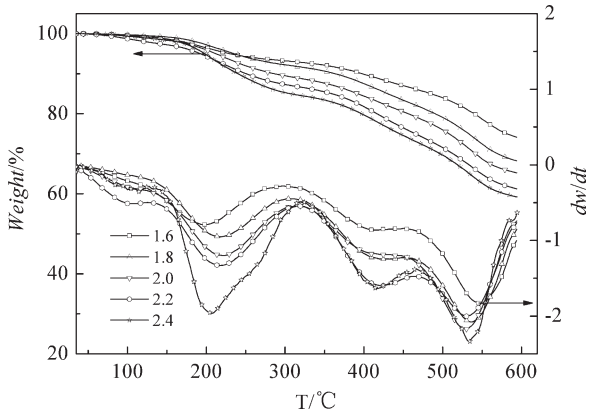

Figure 9. The TGA and DTG curves of HSRPRs using different *F*/*P* molar ratios.

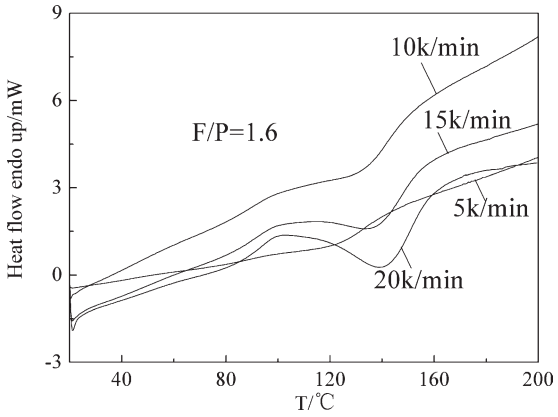

Figure 10. The DSC spectrum of HSRPRs at different heating rates.

activation energy, curing curve on the peak temperature, and heating rate are expressed as follow:

$$-\ln\left(\frac{\beta}{T_p^2}\right) = -\ln\left(\frac{AR}{E_a}\right) + \left(\frac{1}{T_P}\right)\left(\frac{E_a}{R}\right) \quad (1)$$

where β is the heating rate (K/min), T_p is the peak temperature (K), R is the gas constant (8.314 J/(mol K)), and A and E_a are the properties of the material. By plotting $\ln(\beta/T_p^2)$ versus $1/T_p$, obtained a straight line of slope E_a/R, which presented the activation energies of curing reactions.

The curing reaction orders were obtained by plotting ln β versus $1/T_p$ as indicated by the subscripts in Crane equation [eq. (2)].[46]

$$\frac{d(\ln\beta)}{d\left(\frac{1}{T_p}\right)} = -\frac{E_a}{nR} \quad (2)$$

In this study, the DSC curing curves for HSRPRs with $F/P = 1.6$ as a function of the heating rate are shown in Figure 10. There was an exothermic peak in the curing process. This could be attributed to the condensation between the methylol group and hydrogen of benzene ring, forming methylene bridges, and the

Table II. Linear Regression Charts with $-\ln(\beta/T_p^2)$ and $1/T_p$

			Kissinger		
F/*P*	β (K/min)	T_p (°C)	Regression equations	Regression coefficients	R^2
1.6	5	122.63	$y = 11.509x - 18.715$	11.509	0.9988
	10	132.01			
	15	137.49			
	20	140.92			
1.8	5	119.86	$y = 10.932x - 17.453$	10.932	0.9965
	10	130.34			
	15	135.28			
	20	138.86			
2.0	5	116.18	$y = 10.573x - 16.839$	10.573	0.9991
	10	125.75			
	15	130.94			
	20	135.81			
2.2	5	115.32	$y = 9.824x - 15.010$	9.824	0.9958
	10	123.92			
	15	131.23			
	20	135.82			
2.4	5	114.24	$y = 8.976x - 12.885$	8.976	0.9961
	10	123.92			
	15	132.23			
	20	136.19			

Table III. The DSC Data of HSRPRs Using Different F/P Molar Ratios

F/P	β (K/min)	T_p (°C)	ΔH (J g^{-1})	E_a (kJ/mol)	r	n	r′
1.6	5	122.63	27.65	95.69	0.9991	0.9343	0.9992
	10	132.01	30.67				
	15	137.49	30.98				
	20	140.92	32.34				
1.8	5	119.86	41.05	90.88	0.9960	0.9315	0.9965
	10	130.34	29.57				
	15	135.28	35.04				
	20	138.86	36.11				
2.0	5	116.18	67.40	87.90	0.9989	0.9299	0.9991
	10	125.75	30.43				
	15	130.94	38.97				
	20	135.81	12.69				
2.2	5	115.32	39.06	81.68	0.9950	0.9250	0.9958
	10	123.92	40.45				
	15	131.23	29.28				
	20	135.82	11.12				
2.4	5	114.24	67.17	74.63	0.9953	0.9185	0.9961
	10	123.92	17.23				
	15	132.23	12.76				
	20	136.19	15.89				

condensation of two methylol groups, forming dibenzyl ether bridges or the methylene bridges.[26] The plots of $-\ln(\beta/T_p^2)$ against $1/T_p$ for HSRPRs are shown in Table II. The E_a values of HSRPRs as a function of the *F*/*P* molar ratios are shown in Table III. The obtained values of E_a decreased as the *F*/*P* molar ratios increased. Low E_a values indicated that the reaction proceeded fast at a given temperature. This was also confirmed by the gel time of HSRPRs which was shorter with the *F*/*P* molar ratios increasing (Figure 11). These results showed that the reaction speed was quicker, E_a values was lower with the increase of *F*/*P* molar ratios. This might be due to the presence of more reactive sites remaining in the higher molar ratios HSRPRs than those in the lower molar ratio HSRPRs. E_a decreased with the increase of *F*/*P* molar ratios. In other words, a lower E_a value was needed for higher molar ratio, which cured faster than lower molar ratio. In addition, this could be also attributed to the concentration of the methylol groups, which was enhanced with the *F*/*P* molar ratios increasing. This result indicated that increasing the amounts of methylene and ether bridges would make the condensation of the dibenzyl ether bridges more difficult.

Plots of ln β versus $1/T_p$ for HSRPRs are shown in Figure 12, which gave a straight line of slope. Therefore, the reaction orders of curing reactions were obtained. The reaction orders among five different *F*/*P* molar ratios of HSRPRs were calculated, and were non-integer. The result indicated the curing reaction of high-solid content of resol HSRPRs was quite complicated.

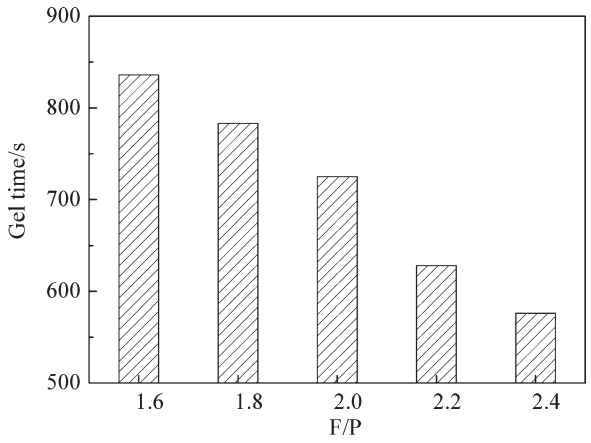

Figure 11. The gel time of HSRPRs of different *F*/*P* molar ratios.

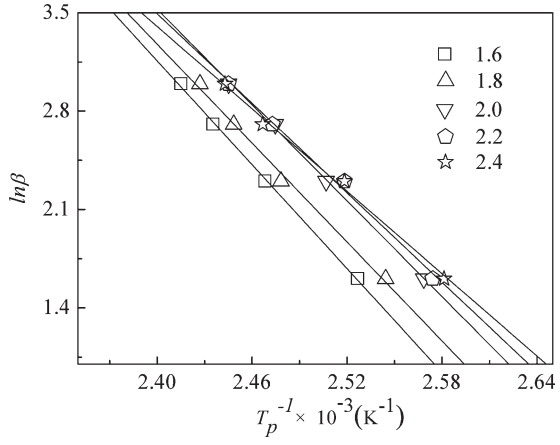

Figure 12. Linear fitting charts with lnβ and $1/T_p$.

CONCLUSIONS

A series of HSRPRs were synthesized, and HSRPRs with best properties were obtained when the *F*/*P* molar ratio was 2.0: the viscosity was 2567 mPa s; solid content was 79.25%; the gel time was 725 s; free formaldehyde content was 0.86%; free phenol content was 3.01%; hydroxymethyl concentration was 36.56%; and the thermal stability was also the highest. The residue (600°C) of HSRPRs decreased when the *F*/*P* molar ratios increased. The low *F*/*P* molar ratios of HSRPRs had higher E_a values than that of high molar ratios. This meant that less heat was needed to cure HSRPRs at high molar ratios than that at low molar ratios. The reaction orders of five different *F*/*P* molar ratios were non-integer, and the result indicated the curing reaction was quite sophisticated. The result had a guiding significance for choosing the right *F*/*P* molar ratios during the manufacturing of HSRPRs.

ACKNOWLEDGMENTS

The work was partially financially supported by National Key Technology Research and Development Program of the Ministry of Science and Technology of China (2012BAD24B04).

REFERENCES

1. Kim, B. G.; Lee, D. G. *J. Mater. Process. Technol.* **2008**, *201*, 716.
2. Lee, S. H.; Teramoto, Y.; Shiraushi, N. *J. Appl. Polym. Sci.* **2002**, *84*, 468.
3. Shen, H. B.; Nutt, S. *Compos. A* **2003**, *34*, 899.
4. Shen, H. B.; Lavoie, A. J.; Nutt, S. R. *Compos. A* **2003**, *34*, 941.
5. Yun, M. S.; Lee, W. I. *Compos Sci Technol* **2008**, *68*, 202.
6. Li, W. L.; Lin, Q.; Yan, M. F.; Zou, Y. S. *J. Appl. Polym. Sci.* **2003**, *90*, 2333.
7. Ma, L. Q.; He, G. Q. *Thermoset. Resin* **2008**, *5*, 24.
8. Ma, L. Q.; He, G. Q. *Technol. Econ. Petrochem.* **2008**, *2*, 11.
9. Liu, Y. F.; Gao, J. G. *Int. J. Chem. Kinetics* **2002**, *11*, 638.
10. Liu, Y. F.; Gao, J. G.; Zhang, R. Z. *Polym. Degrad. Stab.* **2002**, *77*, 495.
11. Park, B.; Riedl, B. *J. Appl. Polym. Sci.* **2000**, *77*, 841.
12. Pizzi, A.; Garcia, R.; Wang, S. *J. Appl. Polym. Sci.* **1997**, *66*, 255.
13. Manfredia, L. B.; de la Osab, O.; Galego Fernández, N.; Vázquez, A. *Polymer* **1999**, *40*, 3867.
14. Liu, X. M.; Guo, Q. *J. China Plast. Ind.* **2007**, *5*, 4.
15. Fu, Z. B. *Appl. Chem. Ind.* **2007**, *1*, 83.
16. Wang, L.; Ren, X. J.; Gao, L.; Zhao, Z. K.; Li, Y. M.; Li, D. F. *Appl. Chem. Ind.* **2009**, *1*, 83.
17. Sun, Z. X.; Wang, L.; Li, D. F. *Eng. Plast. Appl.* **2007**, *11*, 23.
18. Astarloa Aierbe, G.; Echeverría, J. M.; Martin, M. D.; Etxeberria, A. M.; Mondragon, I. *Polymer* **2000**, *18*, 6797.
19. Manfredi, L. B.; Riccardi, C. C.; de la Osa, O.; Vázquez, A. *Polym. Int.* **2001**, *7*, 796.
20. Roczniak, K.; Biernacka, T.; Skarzynski, M. *J. Appl. Polym. Sci.* **1983**, *28*, 531.
21. Holopainen, T.; Alvila, L.; Rainio, J.; Pakkanen, T. T. *J. Appl. Polym. Sci.* **1998**, *69*, 2175.
22. Ebewele, R. O.; River, B. H.; Koutsky, J. A. *J. Appl. Polym. Sci.* **1986**, *31*, 2275.
23. Myers, G. E.; Christiansen, A. W.; Geimer, R. L.; Follensbee, R. A.; Koutsky, J. A. *J. Appl. Polym. Sci.* **1991**, *43*, 237.
24. Solomon, S.; Alfred, R. *J. Appl. Polym. Sci.* **1990**, *41*, 205.
25. Holopainen, H.; Alvila, L.; Pakkanen, T. T.; Rainio, J. *J. Appl. Polym. Sci.* **2003**, *89*, 3582.
26. Holopainen, T.; Alvila, L.; Rainio, J.; Pakkanen, T. T. *J. Appl. Polym. Sci.* **1997**, *66*, 1183.
27. Rego, R.; Adriaensens, P. J.; Carleer, R. A.; Gelan, J. M. *Polymer* **2004**, *45*, 33.
28. He, G. B.; Riedl, B.; Aït-Kadi, A. *J. Appl. Polym. Sci.* **2003**, *89*, 1371.
29. Kim, M. G.; Wu, Y. M.; Amos, L. W. *J. Polym. Sci. Part A: Polym. Chem.* **1997**, *35*, 3275.
30. Luukko, P.; Alvila, L.; Timo, H.; Rainio, J.; Pakkanen, T. T. *J. Appl. Polym. Sci.* **1998**, *69*, 1805.
31. Aierbe, G. A.; Echeverría, J. M.; Riccardi, C. C.; Mondragon, I. *Polymer* **2002**, *43*, 2239.
32. Hong, L.; Pizzi, A.; Despres, A.; Pasch, H.; Du, G. B. *J. Appl. Polym. Sci.* **2006**, *100*, 3075.
33. Huang, R. F.; Wan, L. Q. Phenolic Resin and Its Application; Chemical Industry press: Beijing, **2011**; Chapter 2, p 29.
34. Manfredi, L. B.; de la Osa, O.; Fernández, N. G.; Vázqueza, A. *Polymer* **1999**, *40*, 3867.
35. Carotenuto, G.; Nicolais, L. *J. Appl. Polym. Sci.* **1999**, *74*, 2703.
36. He, G. B.; Riedl, B. *Wood Sci. Technol.* **2004**, *38*, 69.
37. Knop, A.; Pilato, L. Phenolic Resins; Springer-Verlag: New York, **1985**; Chapter 8.
38. Zarate, C. N.; Aranguren, M. I.; Reboredo, M. M. *J. Appl. Polym. Sci.* **2008**, *107*, 2977.
39. Ouyang, Z. H.; Wu, L.; Yi, D. L.; Qin, X. R.; Cao, S. C.; Wang, Y.; Lan, L. *Chem. Ind. Eng. Prog.* **2005**, *8*, 901.
40. Wu, F. C.; Deng, H. F. *J. North China Inst. Sci. Technol.* **2007**, *2*, 29.
41. Blanco, I.; Oliveri, L.; Cicala, G.; Recca, A. *J. Therm. Anal. Calorim.* **2012**, *108*, 685.
42. Blanco, I.; Abate, L.; Bottino, F. A.; Bottino, P. *J. Therm. Anal. Calorim.* **2012**, *108*, 807.
43. Blanco, I.; Abate, L.; Bottino, F. A.; Bottino, P. *Polym. Degrad. Stab.* **2012**, *97*, 849.
44. Blanco, I.; Abate, L.; Bottino, F. A.; Bottino, P.; Chiacchio, M. A. *J. Therm. Anal. Calorim.* **2012**, *107*, 1083.
45. Kissinger, H. E. *J. Res. Natl Bur. Stand.* **1956**, *4*, 217.
46. Crane, L. W.; Dynes, P. J.; Kaelble, D. H. *J. Polym. Sci.: Polym. Lett. Ed.* **1973**, *8*, 533.